

# Reflection and tunneling of ocean waves observed at a submarine canyon

Jim Thomson

WHOI-MIT Joint Program in Oceanography, Woods Hole, Massachusetts, USA

Steve Elgar

Woods Hole Oceanographic Institution, Woods Hole, Massachusetts, USA

T. H. C. Herbers

Naval Postgraduate School, Monterey, California, USA

Received 24 February 2005; accepted 7 April 2005; published 17 May 2005.

[1] Ocean surface gravity waves with periods between 20 and 200 s were observed to reflect from a steep-walled submarine canyon. Observations of pressure and velocity on each side of the canyon were decomposed into incident waves arriving from distant sources, waves reflected by the canyon, and waves transmitted across the canyon. The observed reflection is consistent with long-wave theory, and distinguishes between cases of normal and oblique angles of incidence. As much as 60% of the energy of waves approaching the canyon normal to its axis was reflected, except for waves twice as long as the canyon width, which were transmitted across with no reflection. Although waves approaching the canyon at oblique angles cannot propagate over the canyon, total reflection was observed only at frequencies higher than 20 mHz, with lower frequency energy partially transmitted across, analogous to the quantum tunneling of a free particle through a classically impenetrable barrier. **Citation:** Thomson, J., S. Elgar, and T. H. C. Herbers (2005), Reflection and tunneling of ocean waves observed at a submarine canyon, *Geophys. Res. Lett.*, 32, L10602, doi:10.1029/2005GL022834.

## 1. Introduction

[2] Surface waves with periods between 20 and 200 s (deep water wavelengths between about 500 and 50,000 m) are important to a range of geophysical processes. These infragravity motions are observed in seafloor pressure signals in deep [Webb *et al.*, 1991], coastal [Munk *et al.*, 1956; Tucker, 1950], and nearshore [Guza and Thornton, 1985; Elgar *et al.*, 1992] waters. Recent observations suggest that infragravity waves force resonant oscillations in the earth's crust [Rhie and Romanowicz, 2004], deform ice sheets [Menemenlis *et al.*, 1995], and can be used as proxies to detect tsunamis [Rabinovich and Stephenson, 2004]. Much of the infragravity energy in the ocean is generated nonlinearly by wind waves in shallow water [Longuet-Higgins and Stewart, 1962; Herbers *et al.*, 1995] and reflected seaward at the shoreline [Elgar *et al.*, 1994]. Close to the shoreline, infragravity waves can contain more than 50% of the energy of the wave field [Guza and Thornton, 1985], drive shallow water circulation

[Kobayashi and Karjadi, 1996], and affect shoreline sediment transport and morphological evolution [Guza and Inman, 1975; Werner and Fink, 1993]. Consequently, models for nearshore processes must account for the generation, propagation, and dissipation of infragravity waves. Here, the strong effect of abrupt shallow water topography (Figure 1) on infragravity wave propagation is shown to be consistent with theoretical predictions [Kirby and Dalrymple, 1983], and thus can be included in models for coastal waves, currents, and morphological evolution.

## 2. Theory

[3] The reflection and transmission of long waves ( $L/h \gg 1$ , where  $L$  is the wavelength and  $h$  is water depth) at a long, rectangular submarine canyon of width  $W$  are given by [Kirby and Dalrymple, 1983]

$$R^2 = \frac{\gamma}{1 + \gamma}, \quad T^2 = \frac{1}{1 + \gamma}, \quad (1)$$

and

$$\gamma = \left( \frac{h^2 l^2 - h_c^2 l_c^2}{2hlh_c l_c} \right)^2 \sin^2(l_c W), \quad (2)$$

where  $R^2$  and  $T^2$  are the ratios of reflected and transmitted energy, respectively, to the incident energy, and energy is conserved such that  $R^2 + T^2 = 1$ . The cross-canyon components of the wavenumber vector in water depths within ( $h_c$ ) and outside ( $h$ ) the canyon are given by  $l_c$  and  $l$ , respectively. Assuming Snell's law [Mei, 1989], the along-canyon component ( $m$ ) does not change as waves propagate across the canyon. The dependence of the wavenumber magnitude ( $k = 2\pi/L$ ) on wave radian frequency ( $\omega$ ) and water depth ( $h$ ) is given by the shallow water dispersion relation,  $\omega = k\sqrt{gh}$ , where  $g$  is gravitational acceleration.

[4] When waves arrive nearly perpendicular to the axis of the canyon (i.e., normal incidence), the cross-canyon wavenumber  $l_c = \sqrt{k_c^2 - m^2}$  is real (i.e.,  $k_c > m$ ), and free wave solutions exist both within and outside of the canyon. For normal incidence, the amount of reflection depends primarily on the width of the canyon relative to the wavelength (equation (2)). For example, for a rectangular canyon with  $h = 20$  m,  $h_c = 115$  m, and  $W = 365$  m (similar to La Jolla

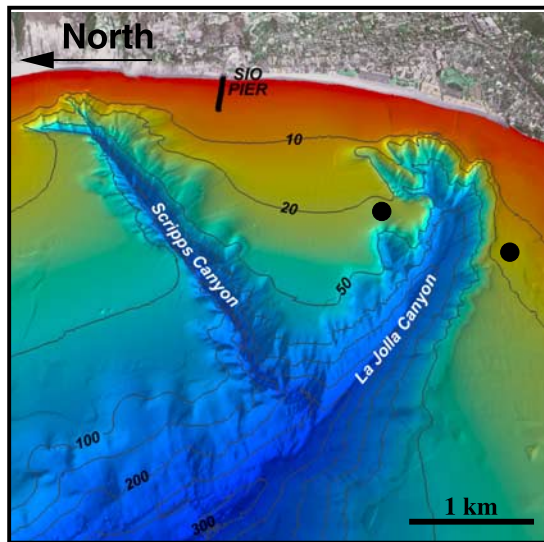


**Figure 1.** Map of underwater bathymetry (curves are depth contours in m below mean sea level) and aerial photograph of the adjacent land near two submarine canyons on the Southern California coast. The Scripps Institution of Oceanography (SIO) pier is between Scripps (the narrow canyon north of the pier) and La Jolla (the wider canyon south of the pier) submarine canyons. The circles on either side of La Jolla submarine canyon are locations of pressure gauges and current meters mounted 1 m above the seafloor for 4 weeks during fall of 2003.

Canyon, Figure 1), equations (1) and (2) predict that reflection increases from zero to half of the incident energy as wavelengths decrease from about 2400 (frequency of 6 mHz) to 600 m (23 mHz) (Figure 2a). Normally incident waves with wavelengths that are integer multiples of twice the canyon width ( $W$ ) are transmitted completely across the canyon (e.g., Figure 2a, where  $R^2 = 0$  and  $T^2 = 1$  for 40 mHz waves [ $L_c \approx 730$  m] normally incident to La Jolla Canyon [ $W = 365$  m]). The absence of reflection is the result of a standing wave pattern between the canyon walls that is in phase with the incident waves, allowing the amplitude at the far side of the canyon to equal the amplitude at the near side of the canyon [Mei, 1989].

[5] In contrast, if waves approach the canyon axis obliquely, defined here as  $k_c < m$ , so that  $l_c = \sqrt{k_c^2 - m^2}$  is imaginary, then no free wave solution exists in the deep water over the canyon, and nearly all the incident energy is reflected (Figure 2b). In the long-wave approximation, the critical angle for total reflection,  $|\theta| = \arcsin(\sqrt{h/hc})$ , is independent of frequency. For the rectangular idealization of La Jolla Canyon (Figure 1),  $|\theta| \approx 25^\circ$ . However, for wavelengths ( $L_c$ ) greater than about 1600 m (i.e., frequencies less than about 20 mHz in Figure 2b), a decaying (i.e., evanescent) wave over the finite-width canyon excites a free wave at the far side of the canyon, resulting in partial transmission of wave energy (Figure 3a).

[6] The reflection and transmission of wave energy at the canyon (Figure 3a) is equivalent to “frustrated total internal reflection” in optics and particle tunneling in quantum mechanics [Krane, 1996, section 5.7]. For example, the solution for the quantum tunneling of a free particle with

energy  $E$  through a potential energy barrier of amplitude  $U$  and width  $W$  (Figure 3b) can be written by replacing equation (2) with

$$\gamma = \frac{U^2}{4E(E-U)} \sin^2\left(\frac{2\pi W}{\lambda}\right), \quad (3)$$

where  $\lambda$  is the de Broglie wavelength of the particle. The resulting reflection and transmission coefficients (equation (1)) describe the probability of observing the particle on either side of the barrier. To the wavelike properties (e.g.,  $\lambda$ ) of the quantum particle, the barrier acts as a one-dimensional finite-width change in refractive medium [Krane, 1996]. When the energy of the particle is greater than the energy of the barrier ( $E > U$ ), the particle may propagate across the barrier, similar to a wave of normal incidence ( $k_c > m$ ) propagating across the canyon. In contrast, when  $E < U$ , the barrier is classically impenetrable, similar to a wave approaching the canyon at an oblique ( $k_c < m$ ) angle. Although a particle with  $E < U$  cannot be observed within the barrier region, there is a nonzero

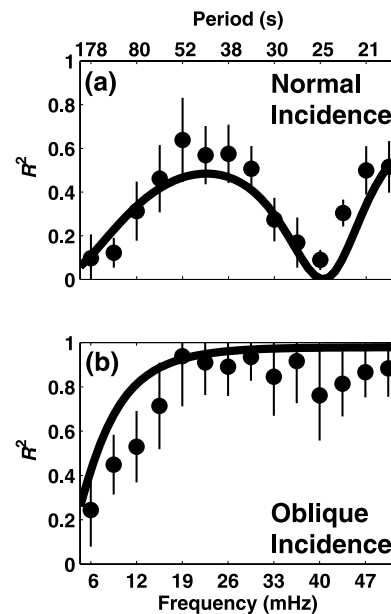


**Figure 2.** Reflection coefficients  $R^2$  versus frequency (mHz) and period (s) for (a) normally and (b) obliquely incident waves. The curves are based on linear long-wave theory [Kirby and Dalrymple, 1983] for a rectangular approximation of the canyon cross-section with depth  $h = 115$  m and width  $W = 365$  m. Theory curves are similar for other rectangular approximations of the canyon profile that preserve the cross-sectional area, and also are similar over the range of angles in each category (i.e., normal and oblique). Circles are the averages of the nonlinear inverse estimates of  $R^2$  at each frequency and vertical lines are  $\pm$  one standard deviation of the estimates. Prior to averaging over cases of normal incidence (typically about 20 cases) or cases of oblique incidence (typically about 30 cases), individual  $R^2$  values are weighted by the narrowness of the corresponding directional spectrum, such that  $R^2$  for narrow directional spectra are weighed more heavily than  $R^2$  for broad spectra.

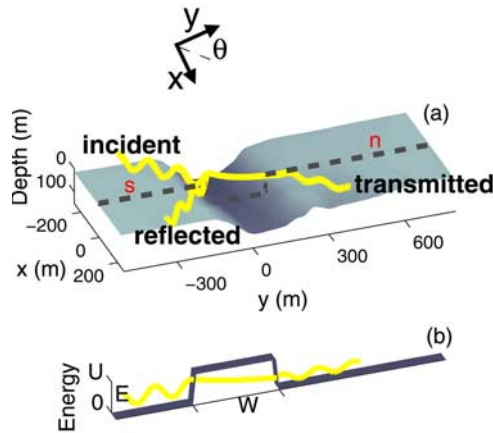


**Figure 3.** Schematic diagrams showing partial reflection of an oblique wave by a submarine canyon and quantum tunneling across an energy barrier. (a) Partial reflection of an obliquely incident wave (yellow curve) over the measured canyon bathymetry (shaded surface). A decaying wave over the canyon excites a transmitted wave on the far side, even though there is no propagation within the canyon. The transmitted wave preserves the angle  $\theta$  relative to the cross-canyon coordinate  $y$ , while the reflected wave reverses the angle. Depth is measured in meters below mean sea level, and a rectangular idealization of the canyon cross-section with  $h = 20$  m,  $h_c = 115$  m, and  $W = 365$  m is shown as a grey dashed line between the south (s) and north (n) instrument sites. (b) Quantum tunneling of a free particle (yellow curve) with energy  $E$  through a finite width  $W$  region of potential energy  $U$ , where  $E < U$  and the region is classically forbidden. The scale of the decaying solution in the forbidden region is set by the de Broglie wavelength of the particle.

probability of observing the particle across the barrier when the de Broglie wavelength ( $\lambda$ ) is large compared to the width of the barrier (analogous to the partial transmission of obliquely incident waves across a finite-width submarine canyon).

### 3. Field Observations

[7] To test equations (1) and (2) in the ocean, measurements of surface-wave-induced pressure and velocity were made with colocated sensors deployed in 20-m water depth (tide range about 1 m) approximately 200 m north and 100 m south of La Jolla Submarine Canyon, near San Diego, California (Figure 1) for 4 weeks during the fall of 2003. Infragravity wave (5 to 50 mHz) significant heights (4 times the sea-surface elevation standard deviation) ranged from 0.01 to 0.20 m. Reflection coefficients were estimated from the 50 (of 327 total) two-hr long time series (sampled at 1000 mHz) with infragravity significant heights greater than 0.05 m at both sides of the canyon.

[8] In contrast to the unidirectional waves used in a laboratory investigation of equations (1) and (2) [Kirby and Dalrymple, 1983], ocean waves can have broad directional distributions that differ on each side of the canyon. The random wave fields on the north (n) and south (s) sides of the canyon consist of incident, reflected, and transmitted

(from the other side of the canyon) waves (Figure 3a), such that the surface elevations  $\eta_s$  and  $\eta_n$  can be written as integrals over wave components at each frequency and direction, given by

$$\eta_s = \int_{\omega} \int_{\theta} d_s \left( e^{i(mx+ly-\omega t)} + R_s e^{i(mx-ly-\omega t+\psi_s)} \right) + d_n \left( T_n e^{i(mx-ly-\omega t)} \right), \quad (4)$$

$$\eta_n = \int_{\omega} \int_{\theta} d_n \left( e^{i(mx-ly-\omega t)} + R_n e^{i(mx+ly-\omega t+\psi_n)} \right) + d_s \left( T_s e^{i(mx+ly-\omega t)} \right), \quad (5)$$

where  $d_s$  and  $d_n$  are the complex-valued differential amplitudes of the incident wave components at radian frequency  $\omega$  and direction  $\theta$  relative to the cross-canyon coordinate  $y$ . The variables  $R_s$ ,  $R_n$ ,  $T_s$ , and  $T_n$  are reflection and transmission coefficients,  $\psi_s$  and  $\psi_n$  are the phase shifts of the reflected waves relative to the incident waves,  $x$  is the along-canyon coordinate, and  $t$  is time. Reflection is assumed to be specular, and thus the sign of the cross-canyon wavenumber ( $l = k \cos \theta$ ) is reversed upon reflection, while the sign of the along-canyon wavenumber ( $m = k \sin \theta$ ) is preserved (Figure 3a).

[9] The observed time series were used to form cross- and auto-spectra of the pressure and velocity associated with the total wave fields observed at each side of the canyon (with a frequency resolution of 3.4 mHz and approximately 42 degrees of freedom). Expressions for the spectra in terms of  $R_s$ ,  $R_n$ ,  $d_s$ ,  $d_n$ ,  $\psi_s$ , and  $\psi_n$  also can be derived from equations (4) and (5) using a linear, hydrostatic momentum balance (appropriate for infragravity waves in 20-m water depth).<sup>1</sup> Assuming energy conservation (i.e.,  $R_s^2 + T_s^2 = 1$ ,  $R_n^2 + T_n^2 = 1$ ), a nonlinear inverse method [Coleman and Li, 1996] was used to solve for the unknown reflection coefficients, directional distributions, and wave phases that yield the cross- and auto-spectra most consistent with the observations (i.e., that minimize a normalized error in fitting the observed spectra at each frequency of each data record). Results were divided into normally ( $k_c > m$ ,  $|\theta| < 20^\circ$ ) and obliquely ( $k_c < m$ ,  $|\theta| > 30^\circ$ ) incident wave fields.

### 4. Results

[10] For waves normally incident to the canyon axis, reflection coefficients estimated with the inverse method are consistent with long-wave theory (Figure 2a), including the nearly complete transmission of waves with wavelength twice the canyon width ( $W = 365$  m,  $L_c \approx 730$  m, frequency = 40 mHz). When unidirectional waves are normally incident on each side of the canyon (i.e., symmetric normal incidence), a forward calculation can be used to estimate reflection, and the few cases that satisfied these criteria also are consistent with long-wave theory (not

<sup>1</sup>Auxiliary material is available at <ftp://ftp.agu.org/apend/gl/2005GL022834>.

shown). Inverse estimates of reflection coefficients for waves obliquely incident to the canyon axis also are consistent with theory, including the nearly complete reflection of waves with frequencies above about 20 mHz, and the tunneling that results in reduced reflection of lower frequency waves (Figure 2b).

[11] The observed reflection of obliquely incident waves is somewhat less than theoretical predictions (Figure 2b), possibly because the neglected non-uniformity of the La Jolla Canyon profile (Figure 1) becomes increasingly important as the incidence angle increases. The reduction in the sharpness of the canyon results in reduced reflection, and also may contribute to the scatter within the reflection coefficients at each frequency band (Figure 2). Directionally spread wave fields that simultaneously contain energy at both normal and oblique angles likely increase the scatter. To reduce this effect, individual reflection coefficients were weighted by the narrowness of the corresponding directional spectrum before averaging (Figure 2). Statistical fluctuations in the cross-spectra of finite-length data records may produce additional scatter [Wunsch, 1996].

[12] Estimates of the phase differences  $\psi_s$  and  $\psi_n$  between incident and reflected waves are consistent with the travel time required for a wave to propagate to the reflector and back, providing a consistency check on the inverse solutions. Further investigation of the reflected wave phase lags could be used to investigate the effect of a spatially distributed reflector (e.g., reflection by sloping, irregularly shaped walls).

[13] During the 4-week observational period, on average more than half the incident infragravity wave energy was reflected by La Jolla submarine canyon. Although low frequency (less than about 20 mHz) waves arriving at angles oblique to the canyon axis cannot propagate within the canyon, a tunneling phenomenon predicts that reflection is only partial (i.e., some energy is transmitted across the canyon), consistent with the observations. These results suggest that reflection of directionally spread waves by complex shallow water bathymetry should be included in models of nearshore processes and considered as a potential shore protection method.

[14] **Acknowledgments.** We thank P. Schultz and the staff of the Center for Coastal Studies, Scripps Institution of Oceanography, for help with the field observations, R. T. Guza for suggestions regarding the inverse

method, and S. Lentz for comments on the manuscript. Funding was provided by the Office of Naval Research and the National Science Foundation. This is Woods Hole Oceanographic Institution contribution number 11324.

## References

- Coleman, T., and Y. Li (1996), An interior, trust region approach for non-linear minimization subject to bounds, *SIAM J. Optim.*, **6**, 418–445.
- Elgar, S., T. H. C. Herbers, M. Okihiro, J. Oltman-Shay, and R. T. Guza (1992), Observations of infragravity waves, *J. Geophys. Res.*, **97**, 15,573–15,577.
- Elgar, S., T. H. C. Herbers, and R. T. Guza (1994), Reflection of ocean surface waves from a natural beach, *J. Phys. Oceanogr.*, **24**, 1503–1511.
- Guza, R. T., and D. Inman (1975), Edge waves and beach cusps, *J. Geophys. Res.*, **80**, 2997–3012.
- Guza, R. T., and E. Thornton (1985), Observations of surf beat, *J. Geophys. Res.*, **90**, 3161–3172.
- Herbers, T. H. C., S. Elgar, and R. T. Guza (1995), Generation and propagation of infragravity waves, *J. Geophys. Res.*, **100**, 24,863–24,872.
- Kirby, J., and R. Dalrymple (1983), Propagation of obliquely incident water waves over a trench, *J. Fluid Mech.*, **133**, 47–63.
- Kobayashi, N., and E. Karjadi (1996), Obliquely incident irregular waves in surf and swash zones, *J. Geophys. Res.*, **101**, 6527–6542.
- Krane, K. (1996), *Modern Physics*, 2nd ed., John Wiley, Hoboken, N. J.
- Longuet-Higgins, M., and R. Stewart (1962), Radiation stress and mass transport in gravity waves, with application to “surf beats,” *J. Fluid Mech.*, **13**, 481–504.
- Mei, C. (1989), *The Applied Dynamics of Ocean Surface Waves*, World Sci., Hackensack, N. J.
- Menemenlis, D., D. Farmer, and P. Czipott (1995), A note on infragravity waves in the Arctic ocean, *J. Geophys. Res.*, **100**, 7089–7094.
- Munk, W., F. Snodgrass, and G. Carrier (1956), Edge waves on the continental shelf, *Science*, **123**, 127–132.
- Rabinovich, A., and F. Stephenson (2004), Longwave measurements for the coast of British Columbia and improvements to the tsunami warning capability, *Nat. Hazards*, **32**, 313–343.
- Rhie, J., and B. Romanowicz (2004), Excitation of Earth’s continuous free oscillations by atmosphere-ocean-seafloor coupling, *Nature*, **431**, 552–556.
- Tucker, M. (1950), Surf beats: Sea waves of 1 to 5 minute period, *Proc. R. Soc. London, Ser. A*, **202**, 565–573.
- Webb, S., X. Zhang, and W. Crawford (1991), Infragravity waves in the deep ocean, *J. Geophys. Res.*, **96**, 2723–2736.
- Werner, B., and T. Fink (1993), Beach cusps as self-organized patterns, *Science*, **260**, 968–971.
- Wunsch, C. (1996), *The Ocean Circulation Inverse Problem*, Cambridge Univ. Press, New York.

S. Elgar, Woods Hole Oceanographic Institution, MS 11, Woods Hole, MA 02543, USA. (elgar@whoi.edu)

T. H. C. Herbers, Naval Postgraduate School, Code OC/He, Monterey, CA 93943, USA. (therbers@nps.edu)

J. Thomson, WHOI-MIT Joint Program in Oceanography, MS 9, Woods Hole, MA 02543, USA. (jthomson@whoi.edu)